Physicochem. Probl. Miner. Process., 58(3), 2022, 145796

http://www.journalssystem.com/ppmp

Physicochemical Problems of Mineral Processing

ISSN 1643-1049

Effect and mechanism of depressant CK102 on flotation separation of fluorite and dolomite

Zhengyao Li [1], Xuewen Wang [1], Chengyan Xu [1], Tichang Sun [1], Weiran Liu [2], Jinzhi Wei [1]

[1] School of Civil and resource Engineering, University of Science and Technology Beijing, Beijing 100083, China

[2] Engineering Company of BGRIMM Technology Group, Beijing 100160, China

Corresponding authors: zyli0213@ustb.edu.cn (Zhengyao Li), chengyan12325@163.com (Chengyan Xu)

Abstract: For a low grade dolomite type fluorite ore in the Hebei province, it was observed that the depressant CK102, a mixture of sulfuric acid, sodium silicate and aluminum sulfate, can effectively inhibit the gangue mineral dolomite in the flotation of fluorite. However, the inhibition mechanism of the depressant is still unclear. In this paper, the flotation separation performance and underlying mechanism of CK102 inhibiting dolomite were investigated through mineral flotation tests, adsorption measurements, infrared spectroscopy, and X-ray photoelectron spectroscopy (XPS). The flotation results showed that the inhibition effect of CK102 on dolomite flotation was much more remarkable than that of fluorite flotation under optimum conditions. Adsorption measurements revealed that there was competitive adsorption between the depressant and collector and that the adsorption of the depressant CK102 prevented the collector modified sodium oleate from adsorbing onto the surface of minerals. The FT-IR and XPS results showed that the co-oxygen cross-linked component of the depressant CK102 chemisorbed on the surface of dolomite; the $CaSiO_3$ precipitation was generated from the reaction of CK102 with Ca^{2+} groups on the surface of the dolomite; $Al_2MgO_8Si_2$ precipitation was also generated from Mg^{2+} reacting with the sodium silicate and aluminum sulfate of CK102. The above adsorptions and reactions enhanced the hydrophilicity of the dolomite surface and the dolomite was effectively depressed.

Keywords: fluorite, dolomite, flotation, depressant CK102, adsorption

1. Introduction

Fluorite (CaF_2) is an important strategic mineral resource. It has been applied in chemical industry, metallurgy, building materials, ceramics, electrical machinery, machinery, medicine, agriculture, precision instruments, etc. It is also an important high-energy material for cutting-edge science and emerging industries (Huang et al.,2017; Li et al., 2015). China has a large reserve of fluorite resources, but much of the resources are low grade. As the new energy, new materials, and other emerging industries develop rapidly, the high grade fluorite resources are further depleted (Cao et al., 2017). and therefore there is urgency to focus on exploitation and utilization of low-grade fluorite resource (Zhang et al., 2018).

Quartz, calcite, barite, celestine and dolomite are the common gangue minerals in low grade fluorite resources. When the gangue mineral is quartz, sodium silicate is often used as a quartz inhibitor for fluorite flotation (Zhang et al., 2003). The inhibition mechanism is that H_2SiO_3 and $HSiO^{3-}$ formed by the dissolution of sodium silicate are adsorbed on the surface of quartz to enhance the hydrophilicity of quartz. When the gangue mineral is calcite/barite/celestite, commonly used inhibitors include modified sodium silicate (Zhou et al., 2013), valonia extract (Ren et al., 2017), citric acid (Gao et al., 2016), sodium fluosilicate (Wang et al., 2020), sodium alginate (Chen et al., 2017), white bark juice (Bulatovic., 2015), tannic acid and starch (GB et al., 2000), polyacrylic acid (Zhang et al., 2018), polycarboxylic acid (Chen et al., 2019), sulfonated lignite (Cui et al., 2020), gelatinous starch (Yang et al., 2020). This type of inhibitor has hydrophilic groups such as -OH, $-NH_2$, -COOH, -CSS, etc., which can be selectively adsorbed on the surface of gangue minerals. When the gangue mineral is dolomite, the inhibitory

DOI: 10.37190/ppmp/145796

mechanism of tannin as a dolomite inhibitor is that the hydroxyl complex $Ca(OH)^+$ formed by the Ca^{2+} on the surface of the dolomite complexes or chelates with the -OH and -COOH in the tannin molecule (Han et al., 2019; Huang et al., 2013;). When sodium silicate is used as a dolomite inhibitor, $HSiO_3^-$ ions, silicic acid molecules and colloidal particles are physically adsorbed on the surface of dolomite to increase its hydrophilicity (Yang et al., 2017). Sodium humate is easy to compete with collectors on the surface of dolomite, and dolomite is inhibited (Nie, 2016). The inhibition effect of depressants combinations is generally better than that of a single depressant. For example, sodium silicate is often used in combination with other depressants to achieve a strong selectivity and inhibition ability (Yu et al., 2017; Zhou et al., 2011; Zhang et al., 2014). Tian Jia et al. used combinations of depressants to inhibit the calcite and celestine, and realized the separation of fluorite (Tian et al., 2019).

In a low grade dolomite type fluorite ore in Hebei Province, the CaF_2 grade is 35.34%, and the gangue mineral is mainly dolomite. The preliminary study of the fluorite mine showed that using sodium humate, tannin, acidified sodium silicate, and sodium fluorosilicate as dolomite inhibitors, respectively, the best index of flotation was CaF_2 grade of 86.23% and recovery rate of 61.20% (Han et al., 2019). Further research found that the inhibitor CK102, a mixture of sulfuric acid, sodium silicate and aluminum sulfate, was recognized with better inhibition effect on dolomite. The fluorite concentrates could be obtained by flotation with CaF_2 grade of 97.62wt% and recovery of 83.69wt% (Liu et al., 2019). The inhibitor CK102 is different from the publicly reported dolomite inhibitors. Even that CK102 has a good inhibitory effect on dolomite in the fluorite flotation, its inhibition mechanism is not clear.

In this paper, through flotation test, adsorption quantity test, infrared spectroscopy (FTIR) analysis and X-ray photoelectron spectroscopy (XPS) analysis, the influence of inhibitor CK102 on the flotation of fluorite and dolomite was studied, and the underlying inhibition mechanism of CK102 on two minerals was investigated. The inhibition mechanism of CK102 provides theoretical support for the flotation separation of fluorite and dolomite.

2. Materials and methods

2.1. Materials

The single mineral samples of fluorite and dolomite used in the experiment were collected from Lingshou County, Hebei Province, China. Through hand selection, crushing, grinding and screening, the minerals samples (-0.074+0.037mm) were used for flotation test, adsorption behavior analysis and XPS test. The X-ray diffractometry and chemical composition of the two powder minerals samples (-0.074 mm) were shown in Fig. 1 and Table 1, respectively. These results showed that the purity of the two minerals is greater than 97wt%. The samples were confirmed to meet the requirements in single-mineral flotation tests and analytical measurement.

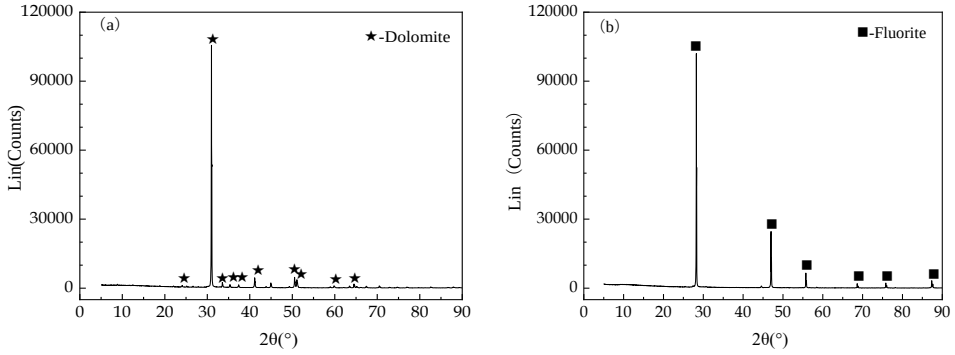

Fig. 1. XRD patterns of the purified samples: (a) dolomite; (b) fluorite

Table 1. Chemical compositions of the purified samples (mass fraction, wt%)

Fluorite	CaF_2	SiO_2
	98.05	1.74
Dolomite	$CaMg(CO_3)_2$	SiO_2
	97.74	1.98

The collector modified sodium oleate is a product of Beijing General Research Institute of Mining and Metallurgy. The depressant CK102 used in the experiment was prepared from sulfuric acid, sodium silicate and aluminum sulfate (quality ratio is 1:4:2). The detailed preparation process was reported as in the references (Liu et al., 2019). Sulfuric acid (H_2SO_4) and sodium hydroxide (NaOH) were used as pH regulators. All of the reagents H_2SO_4, NaOH, modified sodium oleate, Na_2SiO_3 and $Al_2(SO_4)_3$ used in the experiments were of chemical purity.

2.2. Experimental

2.2.1 Flotation tests

Single mineral and artificially mixed minerals flotation tests were carried out on the XFG flotation machine. The effective volume of the flotation tank was 40 cm^3 and the spindle speed of the impeller was 1500 rpm. For single mineral flotation experiments, 2 g of minerals was added to 30 cm^3 of distilled water. For artificially mixed mineral flotation tests, 2 g of mixed mineral was consisted of 1 g fluorite and 1 g dolomite.

The flowsheet for flotation experiments is shown in Fig. 2. The foam products were collected by manual scraping. The scraped foam products and the bottom products of the tank was filtered, dried and weighed, respectively. In single mineral test, the calculated yield was the recovery rate. For artificial mixed minerals t, the CaF_2 grade was measured and the recovery rate was calculated.

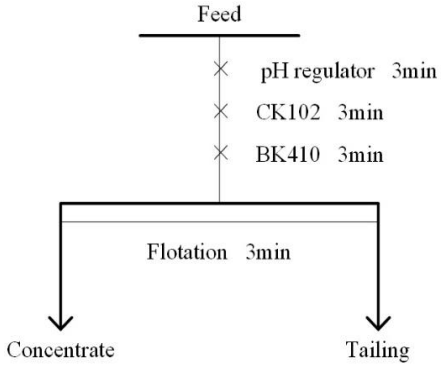

Fig. 2. Flowsheet of single and artificial mixed mineral flotation test

2.2.2. Adsorption measurements

Elementar TOC II instrument (Elementar, Germany) was used for the adsorption experiment. 1g pure mineral (+0.074-0.037mm) and 30mL deionized water were mixed in the beaker. The reagent was added according to the experimental conditions. The magnetic stirrer was used to stir for 90min. The supernatant was centrifuged and used for adsorption measurement. The following equation is used to calculate the amount of modified sodium oleate adsorbed on mineral surface:

$$\tau = \frac{(C_0 - C) \times V}{M \times m} \quad (1)$$

In equation (1), τ is the amount of modified sodium oleate adsorbed on the mineral surface (mol·g^{-1}); C_0 and C are the initial concentration and supernatant concentration of modified sodium oleate (g·L^{-1}), respectively; V is the solution volume (L) after solid-liquid separation; m is the weight of mineral (1g); M is the total molar mass of carbon in modified sodium oleate (g·mol^{-1}).

2.2.3. FT-IR measurements

The infrared spectrum was tested by Ftir-8400s spectrometer (produced by Shimadzu, Japan). The 2 g pure mineral (-0.002 mm) was mixed with 30 mL deionized water in a beaker. The reagent was added according to the test conditions, and the magnetic stirrer was used to stir for 15 min. After repeated washing and filtering with deionized water, the pulp was dried in a vacuum drying oven, and then the infrared test was carried out. The sulfuric acid, sodium silicate, aluminum sulfate and CK102 were

diluted with deionized water to a certain concentration to prepare a solution. The solution was coated on the crystal surface, volatilized and filmed, and then infrared tests were carried out.

2.2.4. XPS measurements

XPS was performed by Kratos AXISULTRADLD (Japan) X-ray photoelectron spectrometer. 2 g pure mineral (-0.002 mm) was mixed with 30 mL deionized water in a beaker. The reagent was added according to the test conditions, and the magnetic stirrer was used for 30 min. After repeated washing and filtering of deionized water, it was put into the vacuum drying box, and then make samples for XPS test. All binding energies were calibrated using the characteristic C1s carbon peak (C1s = 284.7 eV).

3. Results and discussion

3.1. Single and artificial mixed mineral flotation

The influence of pH and reagent concentrations on the flotation recovery of minerals to find the optimum flotation separation conditions was investigated.

Fig. 3 presented the relationship between pH and mineral flotation recoveries using modified sodium oleate as the collector. It was obvious that the pH had a significant influence on the recoveries of fluorite and dolomite. Flotation recoveries of fluorite and dolomite increased sharply with the increase of pH in the range of 6-8. The recovery of fluorite and dolomite reached to 93.74wt% and 91.36wt% respectively at pH 8.0. The recovery of fluorite declined when the pH is higher than 8.0. However, the influence of pH on dolomite was slightly when the pH is higher than 8.0. Good flotation recoveries were obtained for fluorite and dolomite (greater than 80wt%) at pH 6-11. The difference of floatability between fluorite and dolomite was small, and the flotation separation could not be achieved.

Fig. 4 presented the effect of modified sodium oleate concentration on the flotation recovery of fluorite and dolomite. As shown in Fig. 4, flotation recoveries of fluorite and dolomite increased sharply before the concentration of modified sodium oleate reached to 1.5×10^{-4} mol·L^{-1}. At an modified sodium oleate concentration of 1.5×10^{-4} mol·L^{-1}, the recovery of fluorite and dolomite reached to 94.10wt% and 91.52wt%, respectively. The influence of modified sodium oleate concentration on fluorite and dolomite was slightly when the concentration of modified sodium oleate is higher than 1.5×10^{-4} mol·L^{-1}. Without adding other depressant, the flotation behavior of fluorite and dolomite was similar, and the flotation separation of all of them was difficult.

The depressant CK102 was used in the flotation system to accomplish the separation due to the flotation performances of fluorite and dolomite were similar. Fig. 5 presented the flotation recovery of minerals in the presence of the depressant CK102 as a function of pH. Fig. 5 showed that the recovery of fluorite was 87.12wt% at pH 6.0, and then decreased gradually to 68.32wt% at pH 10.0. The results indicated that CK102 had slight inhibition effect on fluorite in the range of pH 6-10. The flotation

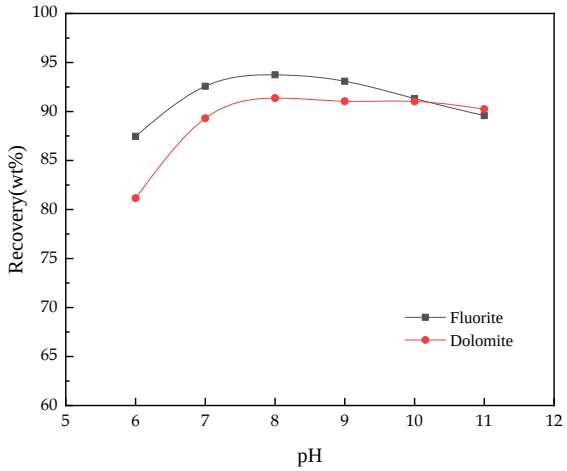

Fig. 3. Recovery of fluorite and dolomite with BK410 as a function of pH values (concentration of modified sodium oleate = 1.5×10^{-4} mol·L^{-1})

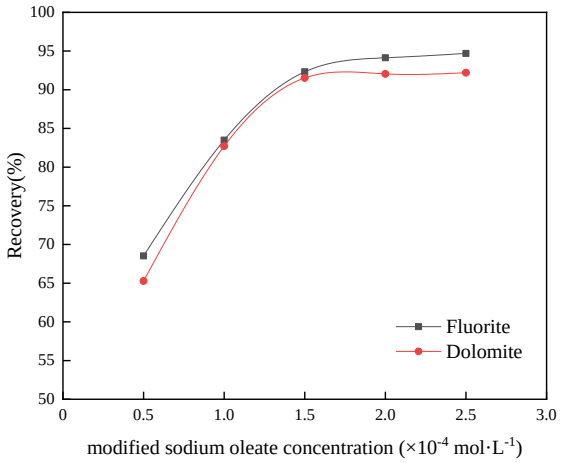

Fig. 4. Effects of the modified sodium oleate concentration on the floatability of fluorite and dolomite (pH = 8)

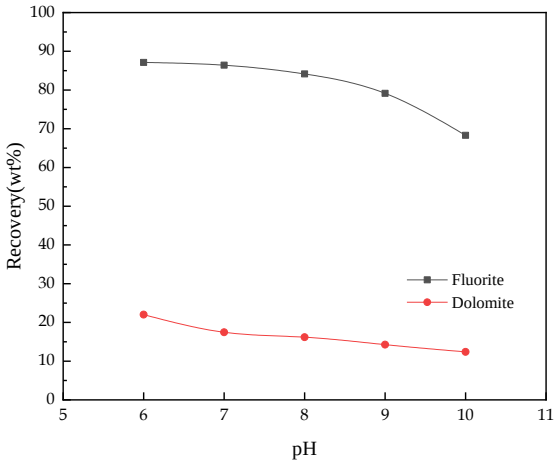

Fig. 5. Recovery of fluorite and dolomite in the presence of the depressant CK102 as a function of pH (concentration of modified sodium oleate = 1.5×10-4 mol·L-1; ρ(CK102) = 20 mg·L-1)

recoveries of dolomite decreased gradually 22.01wt% at pH 6.0 to 12.39wt% at pH 10.0, indicating that CK102 had a good inhibition effect on dolomite under pH 6-10 conditions. The flotation recovery of fluorite reached to 86.43wt% at pH 7.0, while the recovery of dolomite was 17.47wt% at pH 7.0, and the difference in flotation recovery between the two minerals were 68.96wt%. Hence, CK102 can be used as an inhibitor for the effective separation of fluorite and dolomite at pH 7.

Fig. 6 showed that the effect of the depressant CK102 concentration on the floatability of minerals. When the concentration of CK102 increased from 10 mg·L-1 to 50 mg·L-1, the recovery of fluorite decreased gradually from 86.41wt% to 74.94wt%. Within the test range, fluorite exhibited excellent floatability, and the recovery was always higher than 73wt%. When the concentration of CK102 was 10 mg·L-1, the recovery of dolomite was 33.01wt%. With an increase in CK102 concentration (from 10 to 30 mg·L-1), the recovery of dolomite decreased from 33.01wt% to 12.50wt%. Further increase in the CK102 concentration resulted in minor changes in dolomite recovery. It demonstrated that the flotation separation of fluorite from dolomite could be achieved by CK102. Because the flotation recovery difference between fluorite and dolomite was biggest at CK102 concentration of 30 mg·L-1, which was selected for the following experiments.

In order to further verify the selective inhibitory effect of CK102 on dolomite in the process of fluorite flotation, a flotation separation test of binary artificial mixed ore of fluorite and dolomite was carried out. Fig.7 showed that the recovery of fluorite and the grade of CaF_2 in the flotation concentrate were 78.49wt% and 52.27wt% in the absence of CK102. The recovery of fluorite and the grade of CaF_2 in the flotation concentrate were 81.65wt% and 73.26wt% at the CK102 concentration of 30 mg·L-1. It indicated that CK102 could effectively inhibit dolomite in fluorite flotation.

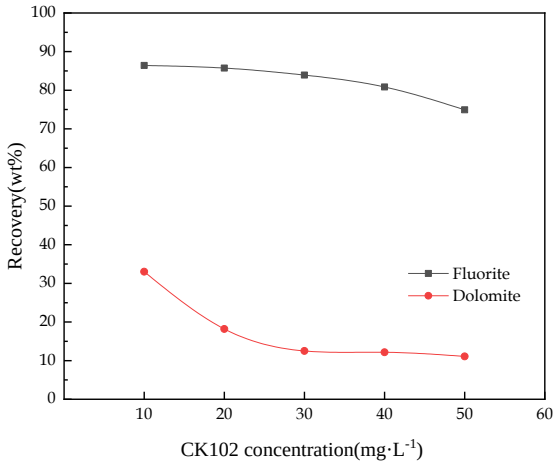

Fig. 6. Effects of the CK102 concentration on the floatability of fluorite and dolomite (concentration of modified sodium oleate = 1.5×10-4mol ·L-1; pH = 7)

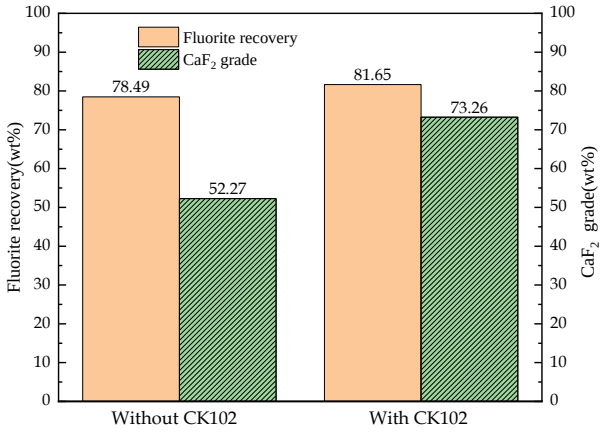

Fig. 7. Effect of CK102 on flotation index of binary mixed ore of fluorite and dolomite (concentration of modified sodium oleate) = 1.5×10-4 mol L-1; ρ(CK102) = 30 mg L-1; pH = 7)

3.2. Adsorption test results

The flotation performance of minerals was directly related with the adsorption behavior. It was great significance that the difference in adsorption of the collector on the surface of the minerals was studied to guide the analysis of flotation separation. Fig. 8 showed the amount of modified sodium oleate adsorbed onto the surface of fluorite and dolomite as a function of the depressant CK102 concentration. Fig. 8 presented that the adsorption of the collector modified sodium oleate on the surface of fluorite and dolomite decreased with an increase in CK102 concentration. The amount of modified sodium oleate adsorbed on the surface of fluorite decreased from 2.62×10-6 mol ·g-1 to 1.53×10-6 mol ·g-1 when the concentration CK102 increased from 0 to 40 mg ·L-1. The amount of modified sodium oleate adsorbed on the surface of dolomite decreased from1.38×10-6 mol ·g-1 to 0.37×10-6 mol ·g-1. At the same time, the amount of the collector modified sodium oleate adsorbed on the surface of fluorite was higher than that on the surface of dolomite. There was competitive adsorption behaviour between the depressant CK102 and the collector modified sodium oleate on the surface of minerals. The adsorption of the depressant CK102 might cover the active sites on the mineral surface and hinder the subsequent adsorption of the collector modified sodium oleate.

3.3. Infrared spectrum results

It can be seen from Fig. 9 and Fig. 10 that in the infrared spectrum of CK102, the antisymmetric stretching vibration peak of −OH was at 3454.27 cm-1, the bending vibration peak of H-OH was at 1639.38 cm-1, and the bending vibration peak of Al-O-Si was at 1104.65 cm-1. Fig. 9 shows that 3582.13

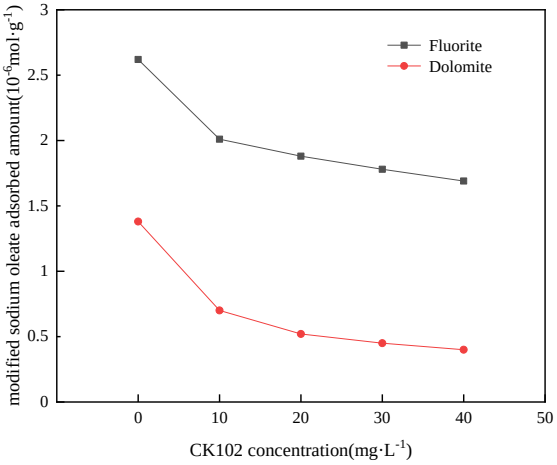

Fig. 8. Amount of modified sodium oleate adsorbed on the surface of minerals as a function of the depressant CK102 concentration (concentration of modified sodium oleate = 1.5×10-4 mol L-1; pH = 7)

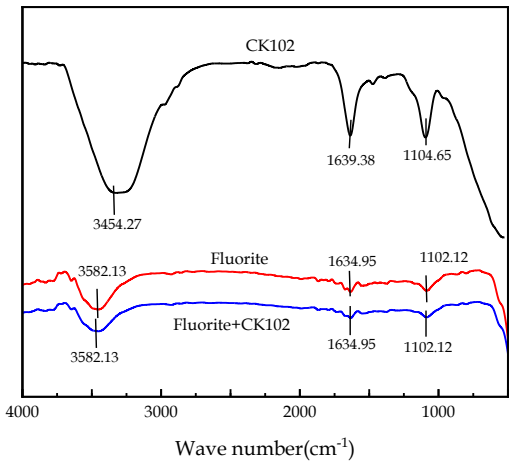

Fig. 9. Infrared spectra of fluorite as a function of CK102

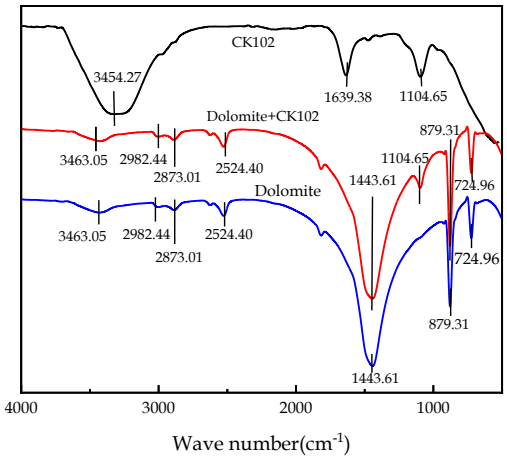

Fig. 10. Infrared spectra of dolomite as a function of CK102

cm-1, 1634.95 cm-1 and 1102.12 cm-1 are the absorption vibration peaks of fluorite. No new absorption peak appeared after the interaction between CK102 and fluorite, indicating that CK102 had physical adsorption on fluorite surface. Fig. 10 shows that the characteristic peaks at 2982.44 cm-1 and 2873.01 cm-1 of the infrared spectrum of dolomite are the first-order frequency doubling peak of the antisymmetric stretching vibration absorption peak of $=CO_3$, the characteristic peak at 2524.40 cm-1 is

the sum frequency peak of the antisymmetric and symmetric stretching vibration of $=CO_3$, the characteristic peak at 1443.61 cm^{-1} is the antisymmetric stretching vibration absorption peak of $=CO_3$, and the characteristic peak at 879.31 cm^{-1} is the out-of-plane bending vibration absorption peak of $=CO_3$. The characteristic peak at 724.96 cm^{-1} is the in-plane bending vibration absorption peak of $=CO_3$. After CK102 acted on dolomite, the bending vibration peak of Al-O-Si appeared at 1104.65 cm^{-1}, where chemical bond cooperation occurred, indicating that CK102 had chemical adsorption on the surface of dolomite.

3.4. Inhibition Mechanism of CK102

The infrared spectra of sulfuric acid, sodium silicate, aluminum sulfate and CK102 were analyzed and as the results were shown in Fig. 11.

As can be seen from Fig. 11, the anti-symmetric stretching vibration peaks of structural water-OH and the bending vibration peaks of H-OH appeared at 3454.27 cm^{-1} and 1639.38 cm^{-1} as a result of that the four reagents were diluted with water in their preparation. In the IR spectra of sulfuric acid, two distinct peaks appeared at 1205.88 cm^{-1} and 1052.67 cm^{-1}, which can be attributed to the bending vibration peak of O-S and the symmetric vibration peak of S=O, respectively. In the IR spectra of sodium silicate, the characteristic peak at 1030.78 cm^{-1} is due to bending vibration peak of Na-O-Si. In the IR spectra of aluminum sulfate, the characteristic peak located at 1106.48 cm^{-1} is corresponding to asymmetric variable-angle vibration peak of $[SO_4]^{2-}$. In the IR spectra of CK102, the characteristic peaks at 1104.65 cm^{-1}, 976.06 cm^{-1} and 613.99 cm^{-1} are respectively assigned to asymmetric variable-angle vibration peak of $[SO_4]^{2-}$, bending vibration absorption peak of Si-OH, and bending vibration peak of Al-OH. Compared to the IR spectra of aluminum sulfate, the $[SO_4]^{2-}$ characteristic peak in the infrared spectrum of CK102 shifted, indicating that part of Al-O-S was transformed into Al-O-Si. Compared to the IR spectra of sodium silicate, the characteristic peak of Si-O in the IR spectrum of CK102 shifted to 976.06 cm^{-1}, which was consistent with the wave number of the bending vibration absorption peak of Si-OH, indicating that some silico-oxygen and aluminum-oxide tetrahedron might be co-oxygenated by non-ionic bonding. The absorption peak at 613-640 cm^{-1} was attributed to the bending vibration of Al-OH and the bending vibration of acid ions and it only appeared in the infrared spectrum of aluminum sulfate and CK102, indicating that AS and CK102 are similar in properties and still belong to the polyhydroxy polymer of aluminum which has a strong hydrophilicity.

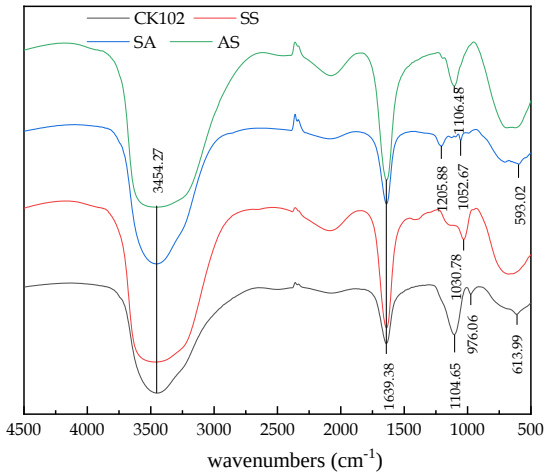

Fig. 11. Infrared spectra of SS, SA, AS and CK102 (Sodium Silicate-SS; Sulfuric Acid-SA; Aluminum Sulfate-AS)

Fig. 12 showed the X-ray photoelectron full spectrum analysis of samples before and after dolomite interacted with CK102 depressant. The elemental calculation results based on the spectrum analysis were shown in Table 2. Results showed that when dolomite was treated by CK102, the XPS peak of Al-O new and characteristic peaks of Al and Si element appeared on the surface; the XPS peak vibration intensity of Ca2p was significantly reduced and the peak position was shifted; the binding energies of element C, element O, and element Ca were all shifted; the content of elements on the dolomite surface

has changed. Fig.11 showed the Al 2p spectrum of dolomite surface before and after treated by CK102. It can be seen from Fig. 13 that when the dolomite was treated by CK102, an obvious peak appeared on the surface at 74.35 eV, which corresponds to the peak level of Al-O. This indicated that chemical adsorption of CK102 occurred on the surface of dolomite which would lead to the hydroxylation of dolomite and enhance the hydrophilicity of dolomite.

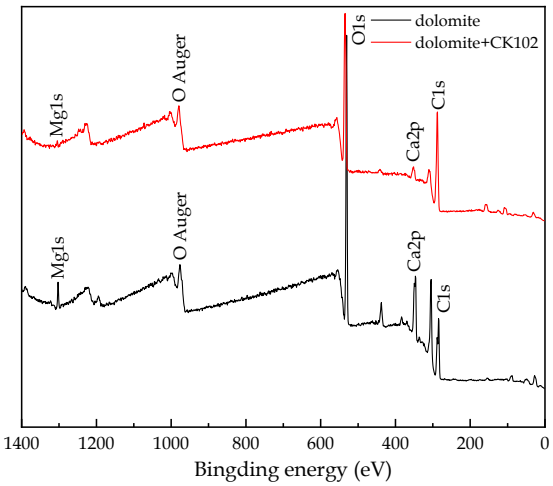

Fig. 12. XPS spectrum of dolomite before and after being treated by CK102

Table 2. Calculation results of XPS element analysis data of dolomite before and after being treated by CK102

Name	Peak BE		FWHM(eV)		Area (P) CPS.(eV)		Atomic(wt%)	
	dolomite	dolomite+ CK102	dolomite	dolomite +CK102	dolomite	dolomite +CK102	dolomite	dolomite +CK102
O 1s	530.95	531.66	3.41	5.42	667229.8	551132.7	48.7	37.75
C 1s	284.8	103.97	4.12	8.12	230212.8	33929.77	40.66	5.6
Mg 1s	1302.8	1284.8	3.24	4.78	60800	331281.4	2.57	54.86
Ca 2p	347.07	348.89	4.19	7.87	261866.8	61662.85	8.07	1.78

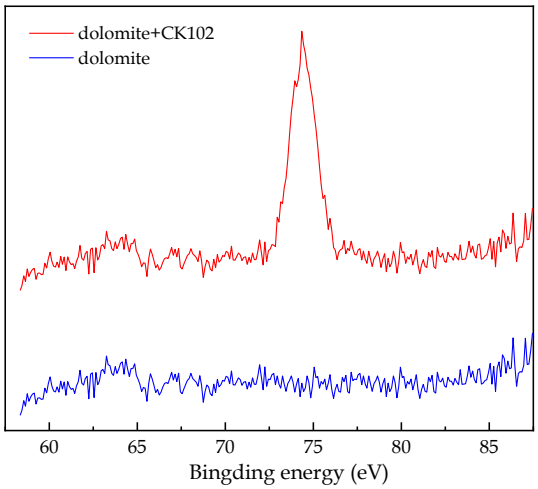

Fig. 13. XPS Al 2p spectrum on the surface of dolomite before and after treated by CK102

In the absence of CK102, there was no Si element on the dolomite surface, while when treated by CK102, the Si element energy spectrum were detected on the dolomite surface by the XPS method. The XPS spectra of Si elements were peaked and fitted as shown in Fig. 14. The calculation results of the Si

elements on the surface of dolomite based on XPS analysis were presented in Table 3. As shown by the analysis, the binding energy of Si 2p3 and Si 2p1 at 98.83 eV and 100.24 eV were consistent with the binding energy of $[O_4Si]^{4-}$, indicating that silicate precipitation was generated on the dolomite surface, which could enhance the hydrophilicity of dolomite surface.

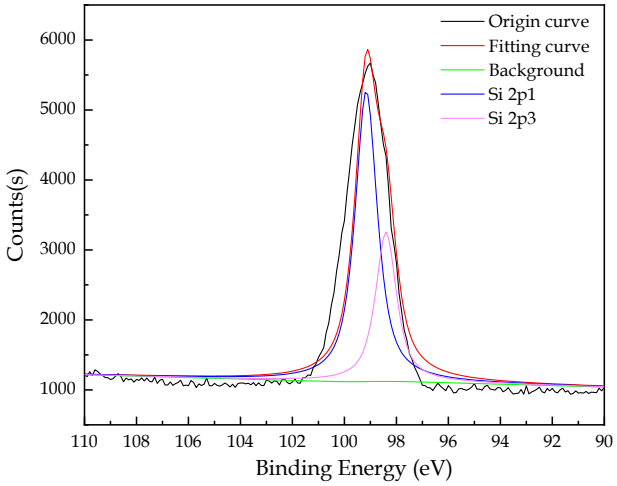

Fig. 14. XPS fitting peaks for Si 2p spectrum on the surface of dolomite before and after being treated by CK102

Table 3. Calculation results of XPS Si element analysis data on the surface of dolomite being treated by CK102

Name	Peak BE	FWHM(eV)	Area (P) CPS.(eV)	Atomic(wt%)
Si 2p3	98.83	2.15	7938.43	69.41
Si 2p1	100.24	1.5	3495.53	30.59

In order to clarify the valence bond morphology of C, O, Ca and Mg on the surface of dolomite before and after treated by CK102, the XPS standard spectral line, manual and database were referred in separating the peaks and fitting the maps. The results were shown in Fig. 15-18 and Table 4-7, respectively.

Fig. 15 showed the C1s narrow-spectrum analysis results before and after dolomite treated by CK102 depressant. In the presence of CK102, the relative content of C=O bonds on the dolomite surface decreased significantly, indicating the decrease of the $[CO_3]^{2-}$ groups. The reason can be attributed to the $[O_4Si]^{4-}$ in CK102 interacted with metal cations on the surface of dolomite.

Fig. 16 presented that the peak of the binding energy of O element was shifted, and three peaks were obtained after peak fitting, among which the binding energy of OH-bond peak, CaO- bond peak and Si-O bond peak were 531.45 eV, 532.45 eV and 530.4 eV, respectively. The photoelectric intensity of OH-bond peak per unit time increased significantly, which indicated that there was a certain hydroxylation phenomenon on the dolomite surface after the addition of CK102. The photoelectric intensity of CaO-bond decreased per unit time, and new Si-O bond peak appeared, indicating the generation of $CaSiO_3$ on the dolomite surface as part of the chemisorption.

The narrow spectrum of Ca2p was shown in Fig. 17. After the addition of CK102, the binding energies of Ca 2p1 and Ca 2p3 were shifted, and the overall trend became lower. The binding energy of $MgCa(CO_3)^{2-}$ peak is greater than that of $CaSiO_3$ peak, which is also consistent with the law that dolomite generates $CaSiO_3$ on the surface after acting with CK102.

Fig. 18 showed the narrow spectrum of Mg 2p. After the addition of CK102, the binding energy of Mg 2p1 and Mg 2p3 were both shifted, and the overall trend became lower. At this point, the binding energy of Mg element was consistent with that of $Al_2MgO_8Si_2$ indicating chemical adsorption on the dolomite surface, and magnesium aluminum silicate precipitation was generated at the same time, resulting in the decrease of the floatability of dolomite.

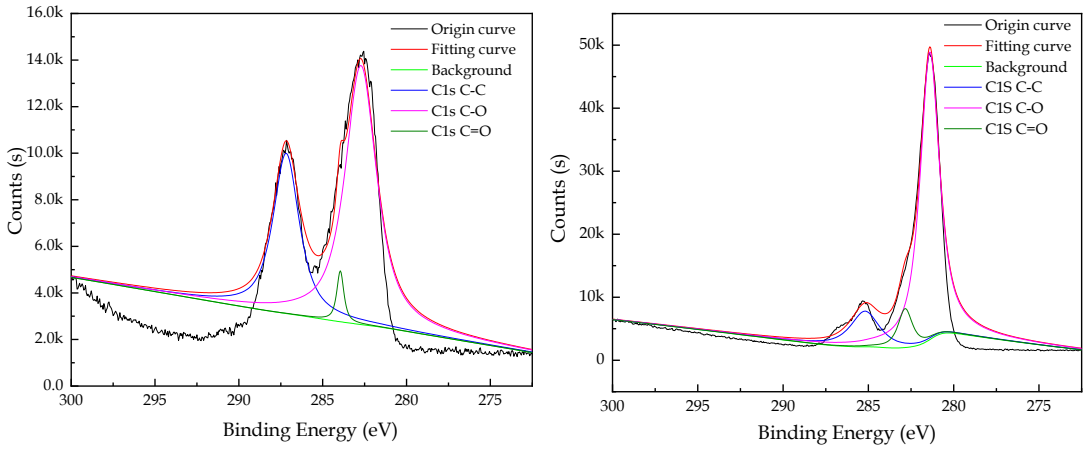

Fig. 15. XPS fitting peaks for C 1s on the surface of dolomite before (left) and after (right) being treated by CK102

Table 4. Calculation results of XPS C element analysis data on the surface of dolomite before and after treated by CK102

Name	Peak BE		FWHM(eV)		Area (P) CPS.(eV)		Atomic(wt%)	
	dolomite	dolomite +CK102	dolomite	dolomite +CK102	dolomite	dolomite +CK102	dolomite	dolomite +CK102
C1s C-C	284.41	281.9	2.88	1.48	40178.86	75248.84	65.08	75.87
C1s C-O	286.36	283.45	1.29	1.23	2617.87	10823.19	4.25	10.92
C1s C=O	289.01	285.8	2.02	1.67	18884.15	13064.39	30.68	13.21

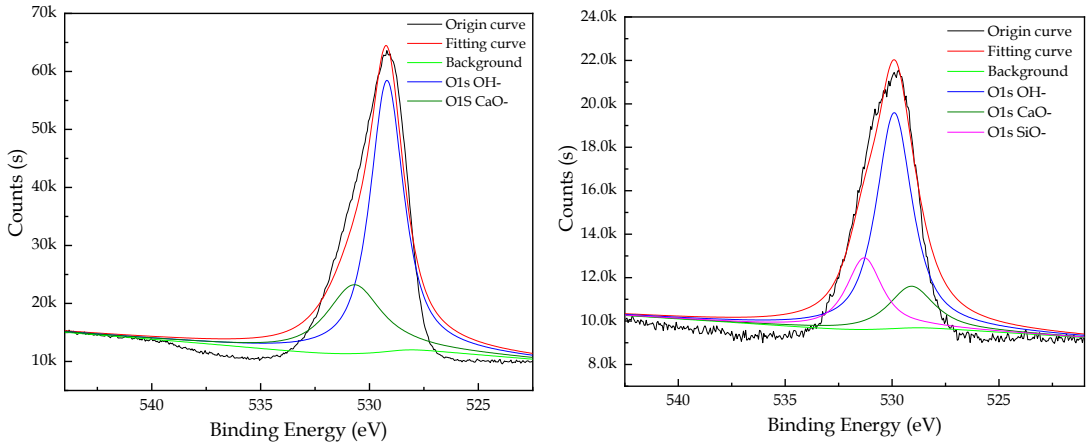

Fig. 16. XPS fitting peaks for O1s on the surface of dolomite before (left) and after (right) being treated by CK102

Table 5. Calculation results of XPS O element analysis data on the surface of dolomite before and after treated by CK102

Name	Peak BE		FWHM(eV)		Area (P) CPS.(eV)		Atomic(wt%)	
	dolomite	dolomite +CK102	dolomite	dolomite +CK102	dolomite	dolomite +CK102	dolomite	dolomite +CK102
O1s OH-	531.06	531.45	3.15	6.53	182826.7	696991.7	93.12	99.13
O1s CaO-	533.51	532.45	1.77	1.13	11723.75	5008.56	5.98	0.71
O1s Si-O	--	530.4	--	2.04	--	1109.1	--	0.16

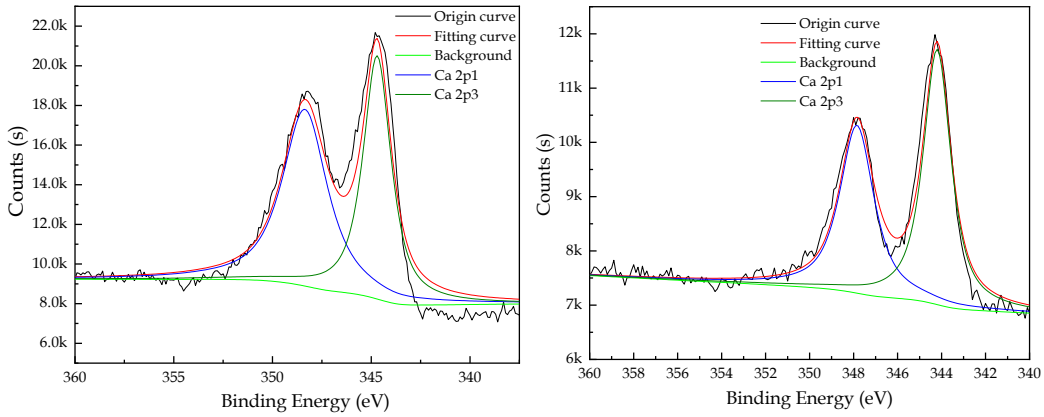

Fig. 17. XPS fitting peaks for Ca 2p on the surface of dolomite before (left) and after (right) being treated by CK102

Table 6. Calculation results of XPS Ca element analysis data on the surface of dolomite before and after treated by CK102

Name	Peak BE		FWHM(eV)		Area (P) CPS.(eV)		Atomic(wt%)	
	dolomite	dolomite +CK102	dolomite	dolomite +CK102	dolomite	dolomite +CK102	dolomite	dolomite +CK102
Ca 2p1	350.16	348.35	2.71	1.93	29589.25	6312.25	41.45	42.28
Ca 2p3	346.66	344.75	2.75	1.61	41899.3	8636.86	58.55	57.72

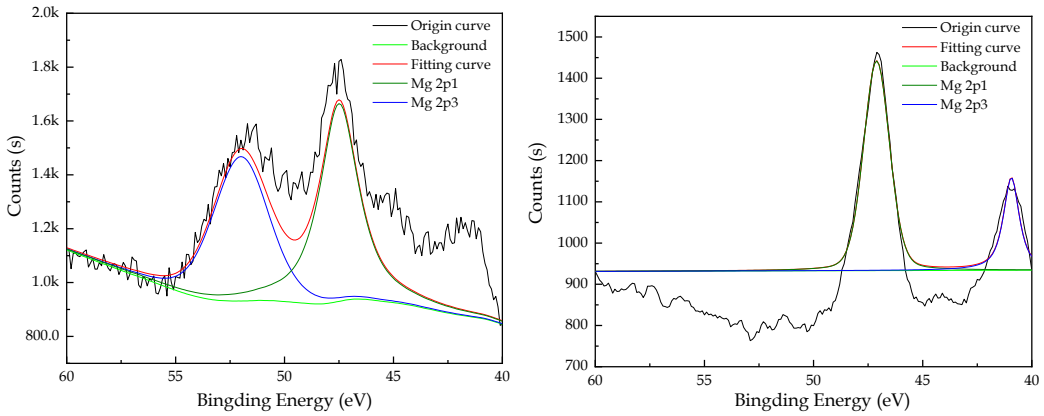

Fig. 18. XPS fitting peaks for Mg 2p on the surface of dolomite before (left) and after (right) being treated by CK102

Table 7. Calculation results of XPS Mg element analysis data on the surface of dolomite before and after treated by CK102

Name	Peak BE		FWHM(eV)		Area (P) CPS.(eV)		Atomic(wt%)	
	dolomite	dolomite +CK102	dolomite	dolomite +CK102	dolomite	dolomite +CK102	dolomite	dolomite +CK102
Mg 2p1	52.36	47.08	0.98	0.91	1504.25	1046.25	41.45	42.28
Mg 2p3	47.01	40.91	1.03	0.72	1339.30	720.86	58.55	57.72

4. Conclusion

CK102 was chemically adsorbed on the surface of dolomite. $[SiO_3]^{2-}$ in CK102 and Ca^{2+} groups on dolomite surface formed $CaSiO_3$ precipitate. $Al_2MgO_8Si_2$ precipitation was also generated from Mg^{2+} reacting with the sodium silicate and aluminum sulfate of CK102. $CaSiO_3$, $Al_2MgO_8Si_2$, and the -OH

group will improve the hydrophilicity of the dolomite surface and hinder the adsorption of modified sodium oleate on dolomite surface. CK102 had physical adsorption on fluorite surface, and had little effect on the adsorption of modified sodium oleate on fluorite surface.

Acknowledgments

This work was financially supported by the National Nature Science Foundation of China (Grant No. 51874017).

References

BULATOVIC, S.M., 2015. Chapter 29. *Beneficiation of Florite Ores.* Elsevier B.V.

CAO, Z.M., YAN, Q., ZHONG, Z.G., ZHU, X.W., 2017. *Status and Prospect of Room Temperature on the Flotation of Fluorite.* Multipurpose Utilization of Mineral Resources. 21-27.

CHEN, C., HU, Y., ZHU, H., SUN, W., QIN, W., LIU, R., GAO, Z., 2019. *Inhibition performance and adsorption of polycarboxylic acids in calcite flotation.* Miner. Eng. 133, 60– 68.

CHEN, W., FENG, Q., ZHANG, G., YANG, Q., ZHANG, C., 2017. *The effect of sodium alginate on the flotation separation of scheelite from calcite and fluorite.* Miner. Eng. 113, 1-7.

CUI, Y.F., JIAO, F., WEI, Q., WANG, X., DONG, L., 2020. *Flotation separation of fluorite from calcite using sulfonated lignite as depressant.* Sep Purif Technol. 242, 116698.

GAO, Z.Y., GAO, Y.S., ZHU, Y.Y., HU, Y.H., SUN, S., SKINNER, W., 2016. *Selective flotation of calcite from fluorite: A novel reagent schedule.* Minerals. 6, 114.

GB, RAJU., S, PRABHAKAR., 2000. *Beneficiation of fluorspar by column flotation.* Mining, Metallurgy & Exploration. 17, 167-172.

HAN, J.C., ZHU, L.X., SUN, T.C., WU, S.C., ZHANG, L., LIU, W.R., 2019. *Comparative Study on the Effect of Low-grade Dolomite-type Fluorite Ore Flotation Inhibitor.* Metal Mine. 8, 102-107.

HUANG, J., ZHANG, C., GUO, Z., 2017. *Research Progress of Fluorite Flotation.* Mod. Min.

LI, L.X., LIU, T., YUAN, Z.T., ZHANG, C., 2015. *The Development in Beneficiation of Fluorite in China.* Conservation and Utilization Of Mineral Resources. 6, 46-53.

LIU, W.R., SUN, T.C., WANG, Y.S., XU, C.Y., ZHU, L.X., 2019. *Research on the Floatation Test of Depressant CK102 in a Low Grade Fluorite Ore.* Non-Metallic Mines. 42, 67-69.

NIE, G.H., 2016.*Selective inhibition and mechanism of fluoride and calcium carbonate minerals*.Beijing University of Science and Technology.

REN, Z.J., YU, F.T., GAO, H.M., CHEN, Z.J., PENG, Y.J., LIU, L.Y., SKINNER, W., 2017. *Selective Separation of Fluorite, Barite and Calcite with Valonea Extract and Sodium Fluosilicate as Depressants.* Minerals. 7, 24.

TIAN, J., XU, L., SUN, W., ZENG, X., FANG, S., HAN, H., HONG, K., Hu, Y., 2019. *Use of $Al_2(SO_4)_3$ and acidified water glass as mixture depressants in flotation separation of fluorite from calcite and celestite.* Miner. Eng. 137, 160-170.

WANG, J., LI, W., ZHOU, Z., GAO, Z., HU, Y., SUN, W., 2020. *1-Hydroxyethylidene-1, 1-diphosphonic acid used as pH-dependent switch to depress and activate fluorite flotation I: Depressing behavior and mechanism.* Chem. Eng. Sci. 214, 115369.

YANG, S.Y., XU, Y.L., LIU, C., HUANG, L., HUANG, Z., LI, H., 2020. *The anionic flotation of fluorite from barite using gelatinized starch as the depressant.* Colloids Surfaces A Physicochem. Eng. Asp 597, 124794.

YANG, K.L., YANG, D.B., WANG, S., ZOU, C., 2017.*Experimental study on flotation of low grade fluorite in Baiyunebo.* Chemical minerals and processing. 46, 29-32.

YU, F.T., SHANG, R.S., YANG, X.J., 2017. *Experimental research on beneficiation of a high calcium-magnesium-quartz type low grade fluorite ore in Sichuan.* Industrial Minerals & Processing. 46, 27-30.

ZHANG, C., GAO, Z., HU, Y., SUN, W., TANG, H., YIN, Z., HE, J., GUAN, Q., ZHU, Y., 2018a. *The effect of polyacrylic acid on the surface properties of calcite and fluorite aiming at their selective flotation.* Physicochem. Probl. Miner. Process. 54, 868–877.

ZHANG, C.H., SUN, W., HU, Y.H., TANG, H.H., YIN, Z.G., GUAN, Q.J., GAO, J.D., 2018. *Investigation of two-stage depressing by using hydrophilic polymer to improve the process of fluorite flotation.* Journal of Cleaner Production. 193, 228-235.

ZHANG, G.F., DENG, H., WEI, K.S., SHI, Q., 2014. *The Effect of Acidized Sodium Silicate on Flotation Separation of Fluorite and Calcite.* Nonferrous Metals (Mineral Processing Section). 1, 80-82.

ZHANG, Y., SONG, S., 2003. *Beneficiation of fluorite by flotation in a new chemical scheme.* Miner. Eng. 16, 597-600.

ZHOU, T., SHI, W.H., 2011. *Experimental Research on the Beneficiation of a High Calcium Fluorite Mine in Jinta County.* Metal Mine. 3, 02-104.

ZHOU, W.B., MORENO, J., TORRES, R., VALLE, H., SONG, S.X., 2013. *Flotation of fluorite from ores by using acidized water glass as depressant.* Miner. Eng. 45, 142-145.